Enhanced sputtering from nanoparticles and thin films: Size effects

Enhanced sputtering from nanoparticles and thin films: Size effects

T. T. Järvi[(a)], J. A. Pakarinen, A. Kuronen and K. Nordlund

Department of Physics, University of Helsinki - P.O. Box 43, FI-00014, Finland, EU

Abstract – Sputtering of gold nanoparticles and nanometer-thin films under 25 keV gallium-ion bombardment is shown, using molecular-dynamics simulations, to be significantly enhanced compared to bulk. The highest yield, about three times that of bulk gold, occurs for particles of about 8 nm in diameter. For thin films, the maximal yield is obtained for roughly 3 nm thick films. A model based on the work of Sigmund is presented to explain the size-dependence.

Introduction. – Ion irradiation can be used to modify the structure of nanoparticles. Light ions, for example, can be used to enhance the magnetic properties of FePt particles due to increased $L1_0$ ordering [1], an effect that is widely used for bulk systems. In some cases, however, nanoparticle systems respond to irradiation quite differently than their bulk counterparts. Multiply twinned FePt and CuAu particles can be transformed to single crystalline morphologies using helium irradiation [2,3], the transformation occuring via intermediate amorphization [4], although neither FePt nor CuAu amorphize in bulk. Heavy ions, on the other hand, can be used to melt, or partially melt, nanoparticles [5].

In all the above applications, where nanoparticles are bombarded with ions, sputtering is an important issue. The large surface-to-volume ratio of particles can be expected to lead to enhanced sputtering compared to bulk surfaces, directly affecting the particle size obtained after irradiation.

Sputtering is even more important in applications such as secondary ion mass spectrometry (SIMS), where gold and silver nanoparticles and thin films deposited onto polymer substrates have been shown to enhance the secondary ion yields from the substrate [6,7]. In this case, the sputtered atoms can directly contribute to the damage produced by the primary ion beam, as well as being visible as secondary ions themselves. Thus for the signal enhancement in SIMS, it is desirable to produce as many secondary metal ions as possible, bringing up the question of optimal particle size.

Despite the need, few previous studies are available on nanoparticles' response to irradiation. The sputtering of ~ 8 nm (diameter) Au clusters under 100 keV Au was studied in ref. [8], while ref. [5] considered He and Xe irradiation of ~ 4 nm Pt particles in the energy range 1–10 keV.

In the present study, we investigate how sputtering is affected by particle size when gold nanoparticles are irradiated with 25 keV gallium ions, a typical ion used in secondary ion mass spectrometry. In addition to nanoparticles, nanometer-thin films are considered, as they also can be used to enhance SIMS signals [6]. Finally, we derive analytic expressions for the size- and thickness-dependence of the sputtering yield to allow the behaviour of other similar systems to be predicted, at least qualitatively.

Methods. – Using molecular-dynamics simulations, we studied 25 keV gallium bombardment of gold nanoparticles and thin films. The interatomic interactions were described using the MD/MC-CEM-formalism [9–11], as it has been shown to reproduce experimental sputtering yields well [12]. At short distances the above potential was smoothly joined to the universal repulsive Ziegler-Biersack-Littmark potential [13] that was also used for the Ga-Au interactions. Inelastic energy losses due to electronic stopping were included in the equations of motion of all atoms with kinetic energy higher than 10 eV [13]. For technical reasons, the stopping was also applied somewhat outside the nanoparticle but this amounted on average to less than $\sim 1\%$ of the total stopping for the incoming ion.

[(a)]E-mail: tommi.t.jarvi@helsinki.fi
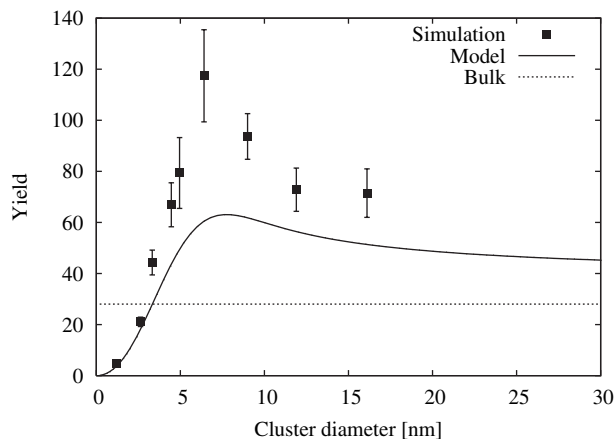
Fig. 1: Sputtering yields of gold clusters under 25 keV Ga bombardment. The horizontal line shows the bulk sputtering yield and the curve gives the prediction of the model described in the text.

The target particles, 1–15 nm in diameter, were created as cuboctahedra and relaxed at 300 K. No substrate was used, as it is desirable to first understand the "pure" response of the particles to irradiation. The particles were rotated randomly prior to bombardment and the ion, impacting along the z-direction, was placed randomly inside a cylinder, the radius of which was chosen equal to the distance of the farthest cluster atom from the geometric center of the cluster. Due to the non-circular cross-section of the clusters, this lead to some ions missing the target. The sputtering yields have been corrected to account for this effect. To gather statistics several hundred simulations were run for each case. The errors presented in figs. 1, 2, and 3 show the standard errors of mean of the results.

Results. –

Molecular dynamics. The sputtering yields of $\sim$1–15 nm gold clusters ($\sim$55–130000 atoms) under Ga bombardment are shown in fig. 1. For small clusters, the sputtering yield is lower than that of bulk gold. The main reason for this is that the ion most often passes through the cluster, only leaving behind a small amount of energy. As the cluster size increases, the energy deposition becomes more efficient, and the sputtering yield increases rapidly. There is a maximal sputtering yield for clusters of around 8 nm in diameter, where the yield is $\sim$3 times that in the bulk. For larger clusters, the yield drops slowly towards the bulk value. It would have been interesting to simulate the sputtering yield beyond the largest, 15 nm, cluster, but the large number of atoms and the required amount of statistics make this impossible with the available computational power.

The general behaviour of the yield as a function of size is easy to understand. The yield obviously has to go down for clusters of just a few atoms and conversely, tend to the bulk yield for large clusters. In the intermediate size
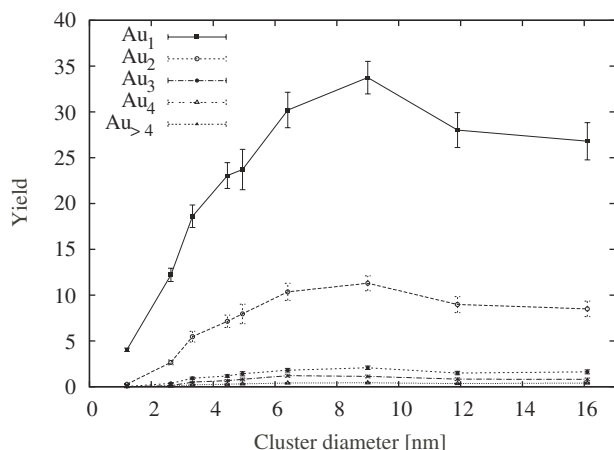
Fig. 2: Cluster sputtering yields of gold clusters under 25 keV Ga bombardment.
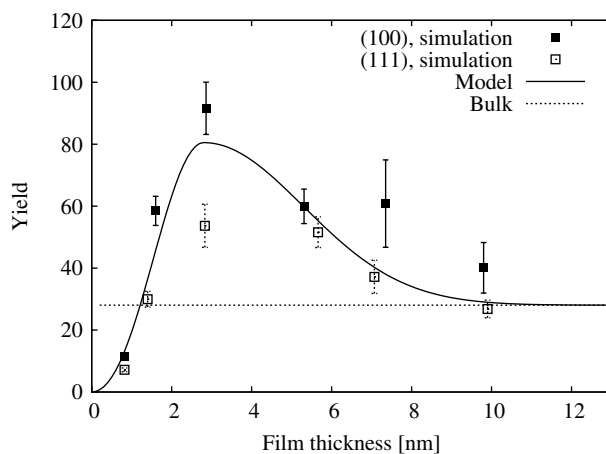
Fig. 3: Sputtering yields of gold films of various thicknesses under 25 keV Ga bombardment. The horizontal line shows the bulk sputtering yield and the curve gives the prediction of the model described in the text.

range the behaviour could either be monotonic or, as it turns out, have a maximum at some size.

The average number of ejected clusters is shown in fig. 2. As expected, mostly monomers and dimers are sputtered, with a small amount of larger clusters.

To compare the cluster sputtering yields with those of bulk matter and nanometer-thin films, we determined the yields for planar (100) and (111) surfaces, as these are the facets appearing in an fcc cuboctahedron. As the bombarded nanoparticles were randomly rotated, the probability of channeling was low and the angle of incidence of the ion oblique. To be able to compare to the bulk results, we thus selected ion impact angles for which little channeling occurs. For the (100)-surface the ion direction, in spherical coordinates, was $(\Theta, \phi) = (25°, 25°)$, while for the (111)-surface, $(6°, 0°)$ was chosen. For bulk targets, the sputtering yields thus obtained were 31 ± 5 and 25 ± 4 for the (100)- and (111)-surfaces, respectively. (The bulk yield shown in figs. 1 and 3 is the average of these two.) For
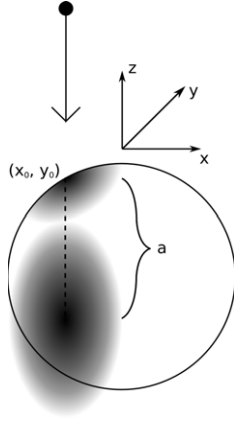
Fig. 4: Schematic of Ga bombardment of a nanoparticle. The damage distribution is centered at depth a below the surface from the impact point.

films of finite thickness, the sputtering yields are shown in fig. 3. For ~ 1 nanometer thin films, the yield is small, again due to the inefficiency of the deposition of energy in the film. As for nanoparticles, the yield increases with film thickness, reaching a maximum value around $\sim 3\,\mathrm{nm}$ films. For thicker films, the yield drops to the bulk value.

Analytical expressions. The enhancement of the sputtering yield compared to bulk can be explained using a model based on the work of Sigmund [14]. The sputtering yield is assumed to be proportional to the damage inflicted on the target surface by the incoming ion. For an arbitrary target surface ∂T, the yield is given by

$$Y_0(r_0) = \Lambda \int_{\partial T} \mathrm{d}^2 r\, F(r, r_0), \qquad (1)$$

where Λ is a proportionality constant, $F(r, r_0)$ is the damage distribution for an ion impacting the surface at r_0, and the integral is over the target surface. The total sputtering yield is then the average of the above expression over the impact point, i.e., $Y = \int \mathrm{d}^2 r_0\, Y_0(r_0) / \int \mathrm{d}^2 r_0$. The model is illustrated in fig. 4.

To simplify the model, the damage distribution is considered independent of the target surface, as suggested by Sigmund [14]. The form of the damage distribution is chosen to be Gaussian, as this has been shown to be a reasonable approximation [15,16]. Hence the distribution is given by

$$F(r, r_0) = \frac{E}{(2\pi)^{\frac{3}{2}} \alpha \beta^2} e^{-\frac{1}{2\alpha^2}[z - h(x_0,y_0) + a]^2}$$
$$\times e^{-\frac{1}{2\beta^2}\left[(x-x_0)^2 + (y-y_0)^2\right]}, \qquad (2)$$

where E is the deposited energy, $r = (x, y, z)$, a gives the depth of the center of the distribution under the impact point, and $h(x_0, y_0)$ is the height of the target surface at the impact point.

For a planar surface, the average over the impact point is redundant as all points are equivalent. Choosing the ion

impact point at the origin, i.e., $r_0 = 0$, and calculating the sputtering yield for a planar surface at $z = d$ using eq. (1) gives

$$Y_{\mathrm{plane}}(d) = \frac{2\pi \Lambda E}{(2\pi)^{\frac{3}{2}} \alpha} e^{-\frac{(d+a)^2}{2\alpha^2}}. \qquad (3)$$

Note that the ion impact point is assumed to be at $z = 0$, regardless of where the planar surface is. Thus, the sputtering yield of a bulk surface is $Y_{\mathrm{plane}}(0)$.

In addition to the constant Λ and the deposited energy E, the parameters in this model are the standard deviations and the depth of the center of the damage distribution, that is, α, β, and a, respectively. The damage distribution can be determined from the bulk bombardment simulations, giving $\alpha = \beta = 2.5\,\mathrm{nm}$ and $a = 2.8\,\mathrm{nm}$. The overall normalization, i.e., the product ΛE, is chosen so that the bulk yield is predicted correctly. We normalize the bulk yield of the model to the average of the yields given above for the (100) and (111) bulk surfaces.

For a film of thickness d, the yield is, as a first approximation, $Y_{\mathrm{plane}}(0) + Y_{\mathrm{plane}}(-d)$. However, this expression only applies when the film is not too thin, as it would imply that as $d \to 0$, the yield would approach twice the bulk yield. This flaw is due to the fact that the effect of the existing surfaces on the damage distribution is neglected. The simplest possible cure for this is to impose a cutoff-function to take the yield to zero. For films thinner than the depth of the damage disribution, a, we multiply the yield by $\sin^2(\frac{\pi z}{2a})$. The resulting curve is shown in fig. 3 and it explains nicely the thickness-dependence of the sputtering yield.

To explain the sputtering yields of the nanoparticles, assume that the clusters are spherical in shape. The sputtering yield for an ion impacting at r_0 is thus, from eq. (1),

$$Y_0(r_0) = \Lambda \int_{S_{2,R}} \mathrm{d}^2 r\, F(r, r_0), \qquad (4)$$

where the integral is over a spherical shell of radius R, centered at the origin, and the impact point in eq. (2) is given by $h(x_0, y_0) = \sqrt{R^2 - x_0^2 - y_0^2}$.

Evaluating eq. (4) gives

$$Y_0(R, \Theta_0) = \frac{2\pi \Lambda E}{(2\pi)^{\frac{3}{2}} \alpha \beta^2} R^2 \int_0^\pi \mathrm{d}\Theta \sin\Theta\, I_0\left(\frac{R^2}{\beta^2} \sin\Theta \sin\Theta_0\right)$$
$$\times e^{-\frac{R^2}{2\alpha^2}\left[\cos\Theta - \cos\Theta_0 + \frac{a}{R}\right]^2 - \frac{R^2}{2\beta^2}\left[\sin^2\Theta + \sin^2\Theta_0\right]}, \qquad (5)$$

where Θ_0 is the polar angle of the ion impact point in spherical coordinates and I_0 is a modified Bessel function [17]. Taking the average over the ion impact point, i.e., integrating over the cross-section of the sphere, gives the total sputtering yield

$$Y_{\mathrm{particle}}(R) = 2 \int_0^{\frac{\pi}{2}} \mathrm{d}\Theta_0 \cos\Theta_0 \sin\Theta_0\, Y_0(\Theta_0). \qquad (6)$$

The integrals can be evaluated numerically. Using the value for ΛE, discussed above, that reproduces the correct bulk yield, eqs. (5) and (6) predict the sputtering yields for nanoparticles shown in fig. 1.

Discussion. – For the larger nanoparticles, the predicted yields are somewhat lower than those obtained by simulation (see fig. 1), but the overall behaviour is the same. This underestimation of the yields is mainly due to the approximation that the existing target surface is not taken into account in the model, and hence for nanoparticles, the Gaussian distribution extends beyond the particle surface. However, the part of the damage distribution outside the target can to some extent be considered as corresponding to the energy reflected from, or transmitted through, the target, although such a correspondence is of course a vague one.

More importantly, the model predicts correctly the particle size and film thickness at which the maximum sputtering yield occurs. For particles, this is at around 8 nm in diameter and for films at a thickness of roughly 3 nm. (see figs. 1 and 3). The maximal yield for particles is significantly higher than that for films. To relate this to the optimal choice for secondary ion mass spectrometry, however, requires further investigation. Especially the damage inflicted on a substrate by the atoms sputtered from the supported particle or film should be assessed. Also the interplay between ballistic sputtering and charge effects should be considered. However, our results suggest that higher SIMS signals may be obtained by using nanoparticles instead of thin film deposition prior to analysis.

Conclusions. – We have investigated the size-dependence of the sputtering yield from 1–15 nm gold particles and thin films. The results show that the yield from particles around 8 nm is enhanced roughly three-fold compared to bulk, a smaller maximal enhancement being observed for films of roughly 3 nm thick. The results can be explained by a model based on Sigmund's sputtering theory. While the model does not reproduce the yields quantitatively, the qualitative behavior is correct. Specifically, the cluster size and film thickness at which maximal sputtering occurs is correctly reproduced.

$$* * *$$

REFERENCES

[1] Wiedwald U., Klimmer A., Kern B., Han L., Boyen H.-G., Ziemann P. and Fauth K., *Appl. Phys. Lett.*, **90** (2007) 062508.
[2] Dmitrieva O., Rellinghaus B., Kästner J., Liedke M. O. and Fassbender J., *J. Appl. Phys.*, **97** (2005) 10N112.
[3] Pohl D., Mohn E., Rellinghaus B., Fassbender J. and Schultz L., unpublished.
[4] Järvi T. T., Pohl D., Albe K., Rellinghaus B., Schultz L., Fassbender J., Kuronen A. and Nordlund K., unpublished.
[5] Järvi T. T., Kuronen A., Nordlund K. and Albe K., *J. Appl. Phys.*, **102** (2007) 124304.
[6] Adriaensen L., Vangaever F. and Gijbels R., *Anal. Chem.*, **76** (2004) 6777.
[7] Marcus A. and Winograd N., *Anal. Chem.*, **78** (2006) 141.
[8] Kissel R. and Urbassek H. M., *Nucl. Instrum. Methods Phys. Res. B*, **180** (2001) 293.
[9] Stave M. S., Sanders D. E., Raeker T. J. and DePristo A. E., *J. Chem. Phys.*, **93** (1990) 4413.
[10] Sinnott S. B., Stave M. S. and Raeker T. J. and DePristo A. E., *Phys. Rev. B*, **44** (1991) 8927.
[11] Raeker T. J. and DePristo A. E., *Int. Rev. Phys. Chem.*, **1991** (10) 1.
[12] Samela J., Kotakoski J., Nordlund K. and Keinonen J., *Nucl. Instrum. Methods Phys. Res. B*, **239** (2005) 331.
[13] Ziegler J. F., Biersack J. P. and Littmark U., *The Stopping and Range of Ions in Matter* (Pergamon, New York) 1985.
[14] Sigmund P., *Sputtering by Ion Bombardment: Theoretical Concepts,* in *Sputtering by Particle Bombardment I,* edited by Behrisch R., *Top. Appl. Phys.*, Vol. **47** (Springer-Verlag) 1981, Chapt. 2, pp. 9–71.
[15] Sigmund P., *Phys. Rev.*, **184** (1969) 383.
[16] Bradley R. M. and Harper J. M. E., *J. Vac. Sci. Technol. A*, **6** (1988) 2390.
[17] Arfken G. B. and Weber H. J., *Mathematical Methods for Physicists* (Academic Press) 1995.